Supplementary Information to "Encoding variable cortical states with short-term spike patterns"

Bartosz Teleńczuk, Richard Kempter, Gabriel Curio, Alain Destexhe

January 4, 2017

1 Generalised linear model

1.1 Methods

One limitation of the spike-train probability model is that the history effects can not extend over the last spike. To evaluate the effects past the last spike we considered the generalised linear model (GLM; Truccolo et al. 2005, Czanner et al. 2015) with conditional intensity $\lambda_{\mathrm{GLM}}(t|\{t_i\})$ of the form

$$\lambda_{\mathrm{GLM}}(t|\{t_i\}) = \exp\left(s(t) + \sum_i h(t - t_i)\right) \tag{1}$$

where $s(t)$ is the driving force and $h(\tau)$ is the spike history kernel.

Note that the intensity function $q(t)$ of the STPM can be identified with $\exp(s(t))$ and recovery function $w(\Delta t)$ with $\exp\left(\sum_i h(t - t_i)\right)$. However, in contrast to the spike-train probability model the effects of the previous spikes can extend infinitely in time. In practice, we reduce the number of free parameters by setting the history horizon above which the spikes can not contribute to the responses any more, such that $h(t > t_{\mathrm{max}}) = 1$. The horizon $t_{\mathrm{max}} = 8$ ms was selected the by means of the Akaike Information Criterion (AIC), which balances the goodness of fit with the number of free parameters of the model.

The likelihood of the GLM is defined analogously to the spike-train probability model:

$$\begin{aligned} L(s; h|\{t_i\}) &= -\int_0^T \lambda_{\mathrm{GLM}}(t_j|\{t_i < t\})dt + \sum_j \ln \lambda_{\mathrm{GLM}}(t_j|\{t_i < t\}) && (2) \\ &= -\int_0^T \exp\left(s(t) + \sum_i h(t - t_i)\right) dt + \sum_j \left(s(t_j) + \sum_i h(t_j - t_i)\right) && (3) \end{aligned}$$

where the sums go over all spikes.

Since the log-likelihood function is a convex function of the parameters, the parameters can be found using standard optimization techniques. In the results presented here we used the conjugate gradient optimization.

We compared the goodness-of-fit of the STPM and the GLM using the time-wrapping method [Brown et al., 2002]: The inter-spike intervals in the experimental data were rescaled to account for temporal variations in firing probability. If the model perfectly reproduced the data the distribution of the rescaled inter-spike intervals would be uniform (the diagonal in Supplementary Figure 1C).

1.2 Results

The STPM and GLM fitted the data almost equally well (Supplementary Figure 1D). They also showed similar goodness-of-fit in terms of the correlation of the residuals with the PSTH (see Figure 1F in the main text).

Increasing the bin size, thus decreasing the number of fitted parameters, degraded the performance of both models, but the GLM deteriorated at a slower rate than the STPM. We found that GLM produced satisfactory results already with a bin size of 0.25 ms (Supplementary Figure 1C, right). With this binning the fitted GLM parameters vary smoothly (Supplementary Figure 1A-B). In particular, the prominent peaks of the PSTH were absent from the intensity function, confirming our hypothesis that these peaks appear due to combination of the high-amplitude intensity function and the refractory period. Importantly, the recovery function displayed oscillations at time scales above 4 ms, which might be related to the adaptation mechanisms or after-hyperpolarising currents (see Conclusions).

We conclude that the input-driven models with spike frequency adaptation spanning several inter-spike intervals [Benda and Herz, 2003] can explain the distribution of the spike patterns in somatosensory cortex.

2 Biophysical model

2.1 Neuron model

Single cortical neuron is represented by a leaky integrate-and-fire (LIF) neuron model whose membrane potential dynamics is described by:

$$C_m \frac{dV}{dt} = -g_L(V - V_{\text{rest}}) - I_{\text{syn}}(V, t) \tag{4}$$

where C_m is membrane capacitance, g_L is the leak conductance, V_{rest} is the resting potential and I_{syn} are the synaptic currents (described below). When the membrane potential reaches the threshold V_{thr} a spike is generated and the potential is reset to V_{reset} putting the cell into a hyperpolarised state.

2.2 Intracortical inputs

The LIF neuron receives horizontal inputs from other cortical cells and feedforward inputs from the thalamus. The cortical inputs consist of n_{exc} excitatory and n_{inh} inhibitory fibers which are tonicaly active with constant firing rate $f_{\text{exc}} = f_{\text{inh}}$. The input spike trains are generated from Poisson distribution. Each spike results in a transient increase of the synaptic conductance which is given exponential function:

$$g_i(t - t_{sp}) = \begin{cases} w_i \exp((t - t_{sp}))/\tau_i), & t - t_{sp} \geq 0 \\ 0, & t - t_{sp} < 0 \end{cases}, i = \text{exc, inh} \tag{5}$$

where w_{inh} and w_{exc} are the inhibitory and excitatory synaptic weights, τ_{exc} and τ_{inh} stand for the synaptic time constants, t_{sp} is the arrival time of the presynaptic spike. The inhibitory and excitatory synaptic weights are adjusted to achieve approximate balance between excitation and inhibition [Destexhe et al., 2003, Shadlen and Newsome, 1998].

The synaptic current contributed by intracortical connections is defined by:

$$I_{\text{Cortex}} = g_{\text{exc}}(t)(V - E_{\text{exc}}) + g_{\text{inh}}(t)(V - E_{\text{inh}}) \tag{6}$$

where $g_{\mathrm{exc}}(t)$ and $g_{\mathrm{inh}}(t)$ are synaptic conductances and E_{inh} and E_{exc} are the reversal potentials of inhibitory and excitatory synapses respectively.

2.3 Thalamocortical inputs

The LIF neuron receives also n_{Th} excitatory inputs from the thalamus. In contrast to intracortical inputs, they are assumed to be activated only after presenting the stimulus and are silent before that. The post-stimulus activity in each thalamocortical fiber is modelled by a Poisson process with the constant firing rate f_{Th}.

The efficiency of thalamocortical synapses is assumed to be modulated by their activity. This phenomenon called short-term synaptic depression (STSD) was shown to take place in intracortical and thalamocortical synpases. Here, we employed a phenomenological description of STSD developed by Tsodyks and Markram [1997] with subsequent adaptations to conductance-based synapses. In the model, the effective synaptic strength is determined by the factor y_i, which evolves according to the equations:

$$\frac{dx_i}{dt} = \frac{z_i}{\tau_{rec}} - Ux_i\delta(t - t_{\mathrm{sp}}) \tag{7}$$

$$\frac{dy_i}{dt} = Ux_i\delta(t - t_{\mathrm{sp}}) \tag{8}$$

$$\frac{dz_i}{dt} = \frac{y_i}{\tau_1} - \frac{z_i}{\tau_{\mathrm{rec}}} \tag{9}$$

where τ_1 is the decay constant of synaptic conductance, τ_{rec} is the recovery time from synaptic depression and U describes the fraction of available resources used by each presynpatic spike.

The postsynaptic current due to the thalamocortical inputs is then:

$$I_{\mathrm{Th}} = G_{\mathrm{Th}}(t)(V - E_{\mathrm{exc}}), \tag{10}$$

and

$$G_{\mathrm{Th}}(t) = \sum_{i=1}^{n_{\mathrm{Th}}} y_i(t) g_{\mathrm{Th},i}(t) \tag{11}$$

where G_{Th} is the total conductance due to thalamic inputs, $g_{\mathrm{Th},i}$ stands for conductance of a single synapse and y_i its efficiency. The contribution of a single presynaptic spike to postsynaptic conductance is assumed to be the same as for an excitatory cortical synapse (i.e. $g_{\mathrm{exc}}(t)$).

The total synaptic current in the LIF neuron is a sum of intracortical and thalamocortical currents: $I_{\mathrm{syn}}(t) = I_{\mathrm{Cortex}}(t) + I_{\mathrm{Th}}(t)$.

2.4 Parameter fitting

All of the fixed and adjustable parameters are listed in SupplementarySupplementary Table 1. We used Monte Carlo method to generate responses of the cell to repeated stimulations. To this end, we ran the model simulations 500 times, each time obtaining the timings of action potentials (spike trains). From these responses we calculated post-stimulus time histogram (PSTH) and compared it to experimental data. The parameters of the model were fitted by means of evolutionary approach (Differential Evolution) and manually tuned to obtain the minimum difference between real and simulated PSTH.

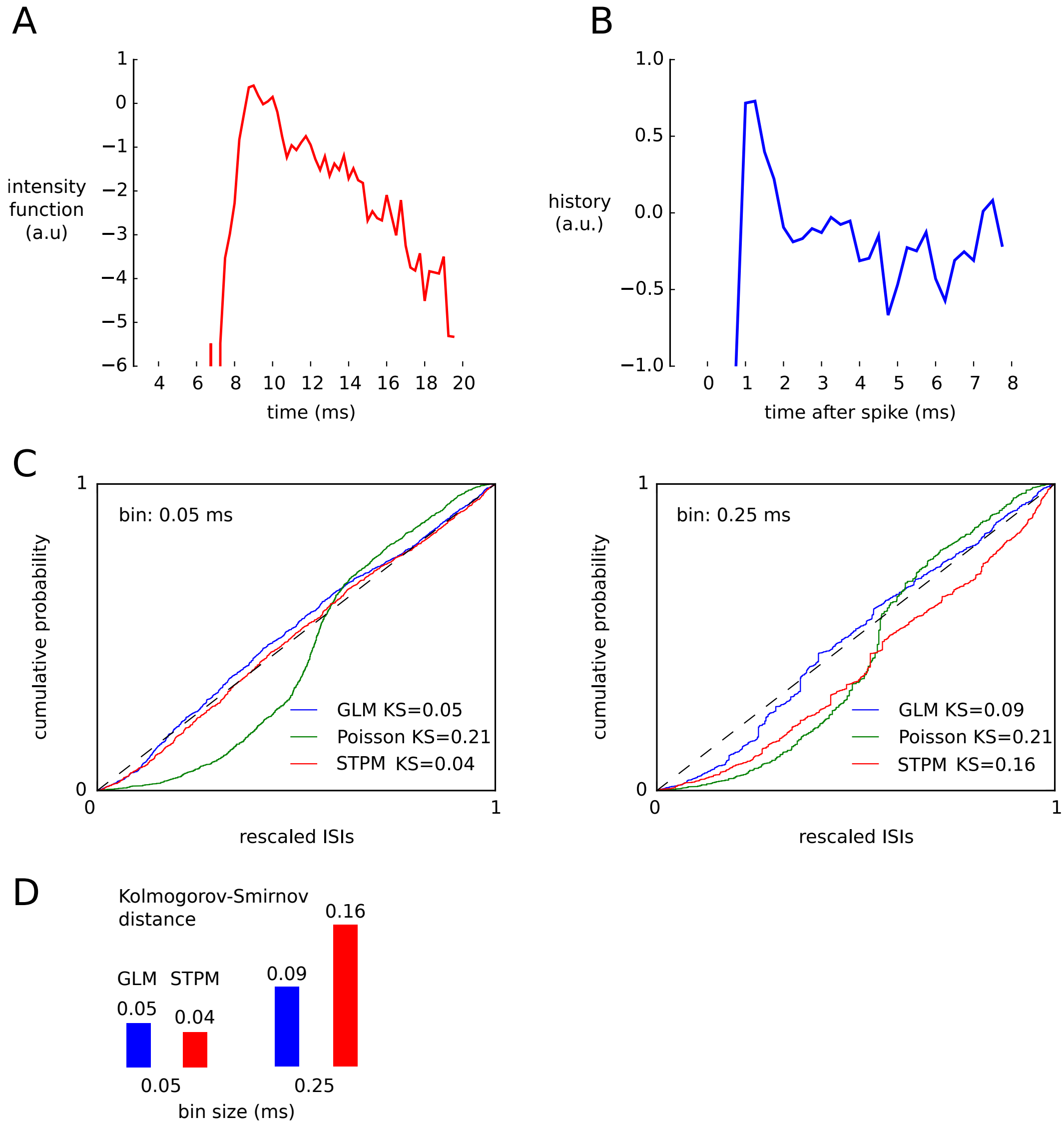

Supplementary Figure 1: The generalised liner model (GLM) with time-varying firing rate and history effects. (**A**) The intensity function of the GLM (bin size 0.25 ms) characterises the time-dependence of the firing rate, which is modulated by synaptic inputs. The intensity function rises rapidly, but decays smoothly. Importantly, it does not follow the prominent peaks visible in the PSTH. (**B**) The history filter characterising the refractoriness. The filter consists of an absolute refractory period of 0.5 ms (strongly negative values were clipped) followed by a relative refractory period and an over-shoot (spike facilitation). (**C**) Goodness-of-fit test based on time-rescaling theorem. Inter-spike intervals of the experimental spike trains were rescaled according to the conditional intensity function of three models: Poisson, spike-train-probability model (STPM), generalised linear model (GLM). If the model perfectly reproduced the data the inter-spike intervals would be distributed uniformly on 0-1 interval (diagonal). The difference between the theoretical and the empirical distributions was evaluated by means of Kolmogorov-Smirnov statistics (K-S). This procedure was repeated for two different bin sizes (0.25 ms, left; and 0.05 ms, right). (**D**) The goodness-of-fit, as measured by the Kolmogorov-Smirnov distance (maximum divergence from diagonal in C), decreased with bin size in both STPM and GLM, but the decrease was slower for GLM.

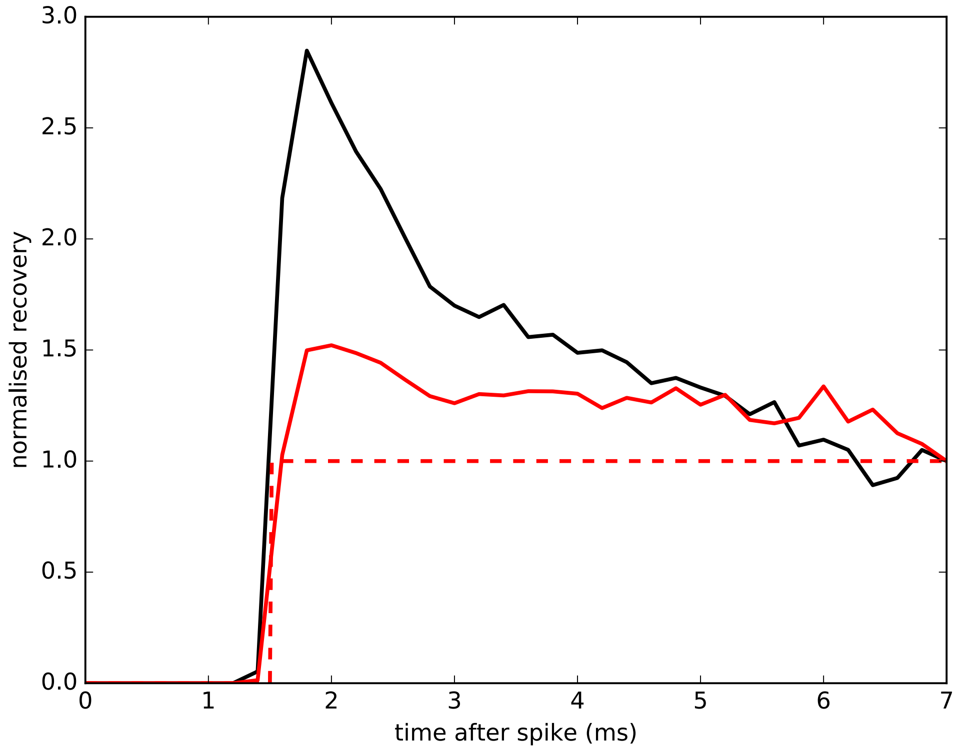

Supplementary Figure 2: Recovery function estimated from simulated spike trains with (solid black line) and without (solid red line) trial-to-trial gain modulation. The spike trains were generated with exponentially decaying intensity function $4000\,\mathrm{Hz} \times \exp[-t/(5\,\mathrm{ms})]$ and a step-like recovery function (dashed red line). The overshoot appearing after the absolute recovery period ($\tau_{\mathrm{ref}} = 1.5$ ms) is an artifact of the trial-to-trial variation and not a marker of a genuine spike facilitation mechanism. The estimated recovery functions were normalised by dividing them with their value at time $t = 7\,\mathrm{ms}$. The trial-to-trial variations were simulated as in the population model described in main text where G was drawn independently for each trial from an uniform distribution on the interval [0.2, 0.8].

Parameter	Symbol	Units	Value	References
LIF neuron:				
– membrane capacitance	C_m	nF	0.5	Johnston and Wu [1995]
– leak conductance	g_L	μS	0.025	Johnston and Wu [1995]
– rest potential	V_{rest}	mV	-70	Johnston and Wu [1995]
– spike threshold	V_{thr}	mV	-40	Johnston and Wu [1995]
– reset potential	V_{reset}	mV	-70	Johnston and Wu [1995]
Cortical excitatory inputs:				
– synaptic weight	w_{exc}	μS	0.0072 (*)	
– synaptic time constant	τ_{exc}	ms	0.9 (*)	Stern et al. [1992]
– synaptic reversal potential	E_{exc}	mV	0	Johnston and Wu [1995]
– number of connections	n_{exc}	–	200	Douglas and Martin [2007]
– firing rate	f_{exc}	Hz	10 (*)	
Cortical inhibitory inputs:				
– synaptic weight	w_{inh}	μS	0.022 (*)	
– synaptic time constant	τ_{inh}	ms	4	Johnston and Wu [1995]
– synaptic reversal potential	E_{inh}	mV	-70	Johnston and Wu [1995]
– number of connections	n_{inh}	–	n_{exc}	Douglas and Martin [2007]
– firing rate	f_{inh}	Hz	f_{exc}	
Thalamocortical inputs:				
– synaptic weight	w_{Th}	μS	0.035 (*)	
– time constant	τ_{Th}	ms	τ_{exc}	
– reversal potential	E_{Th}	mV	E_{exc}	
– number of connections	n_{Th}	–	28 (*)	Douglas and Martin [2007]
– firing rate	f_{Th}	Hz	700 (*)	Hanajima et al. [2004]
– use of synaptic resources	U	–	0.6 – 0.9 (*)	Gil et al. [1997, 1999]
– decay of synaptic conductance	τ_1	ms	τ_{exc}	
– recovery time	τ_{rec}	ms	700	Gil et al. [1997]

Supplementary Table 1: List of parameters used in the leaky integrate-and-fire model. "Value" column indicates typical parameter values or ranges found in the literature (where available). (*) denotes the parameters which were adjusted to fit the experimental data.

References

J. Benda and A. V. M. Herz. A universal model for spike-frequency adaptation. *Neural Comput.*, 15(11):2523–2564, 2003.

E. N. Brown, R. Barbieri, V. Ventura, R. E. Kass, and L. M. Frank. The time-rescaling theorem and its application to neural spike train data analysis. *Neural Comput.*, 14(2):325–346, 2002.

G. Czanner, S. V. Sarma, D. Ba, U. T. Eden, W. Wu, E. Eskandar, H. H. Lim, S. Temereanca, W. A. Suzuki, and E. N. Brown. Measuring the signal-to-noise ratio of a neuron. *Proc. Natl. Acad. Sci. U. S. A.*, 112(23):7141–7146, 2015. doi: 10.1073/pnas.1505545112.

A. Destexhe, M. Rudolph, and D. Paré. The high-conductance state of neocortical neurons in vivo. *Nat. Rev. Neurosci.*, 4(9):739–751, 2003.

R. J. Douglas and K. A. C. Martin. Mapping the matrix: the ways of neocortex. *Neuron*, 56(2): 226–238, Oct. 2007. ISSN 0896-6273. doi: 10.1016/j.neuron.2007.10.017.

Z. Gil, B. Connors, and Y. Amitai. Differential regulation of neocortical synapses by neuromodulators and activity. *Neuron*, 19(3):679–686, 1997.

Z. Gil, B. Connors, and Y. Amitai. Efficacy of thalamocortical and intracortical synaptic connections: quanta, innervation, and reliability. *Neuron*, 23(2):385–397, 1999.

R. Hanajima, R. Chen, P. Ashby, A. M. Lozano, W. D. Hutchison, K. D. Davis, and J. O. Dostrovsky. Very fast oscillations evoked by median nerve stimulation in the human thalamus and subthalamic nucleus. *J. Neurophysiol.*, 92(6):3171–3182, 2004.

D. Johnston and S. Wu. *Foundations of cellular neurophysiology.* MIT Press, Cambridge, USA, 1995.

M. Shadlen and W. Newsome. The variable discharge of cortical neurons: Implications for connectivity, computation, and information coding. *J. Neurosci.*, 18(10):3870–3896, 1998.

P. Stern, F. A. Edwards, and B. Sakmann. Fast and slow components of unitary EPSCs on stellate cells elicited by focal stimulation in slices of rat visual cortex. *J. Physiol. (Lond.)*, 449: 247–278, 1992.

W. Truccolo, U. T. Eden, M. R. Fellows, J. P. Donoghue, and E. N. Brown. A point process framework for relating neural spiking activity to spiking history, neural ensemble, and extrinsic covariate effects. *J. Neurophysiol.*, 93(2):1074–1089, 2005.

M. Tsodyks and H. Markram. The neural code between neocortical pyramidal neurons depends on neurotransmitter release probability. *Proc. Natl. Acad. Sci. U. S. A.*, 94(2):719–723, 1997.